Yizengaw Endawoke (Orcid ID: 0000-0001-5772-3355)
Zesta Eftyhia (Orcid ID: 0000-0002-1899-5275)
Moldwin Mark, B. (Orcid ID: 0000-0003-0954-1770)
Magoun Matt, S. (Orcid ID: 0000-0001-9949-6955)
Surussavadee Chinnawat (Orcid ID: 0000-0003-2734-8907)
Bbamba Zoumana (Orcid ID: 0000-0002-8913-3357)

ULF Wave Associated Density Irregularities and Scintillation at the Equator

E. Yizengaw[1], E. Zesta[2], M. B. Moldwin[2], M. Magoun[1], N. K. Tripathi[4], C. Surussavadee[5], and Z. Bamba[6]

[1]Institute for Scientific Research, Boston College, Boston, USA; [2]NASA Goddard Space Flight Center, Greenbelt, Maryland, USA; [3]Climate and Space Sciences and Engineering, University of Michigan, Ann Arbor, USA; [4]Remote Sensing and GIS, School of Engineering and Technology, Asian Institute of Technology, Bangkok, Thailand; [5]Faculty of Engineering, King Mongkut's Institute of Technology Ladkrabang, Bangkok, Thailand; [6]Centre de Recherche Scientifique de Conakry Rogbanè, Conakry, Guinea.

Abstract: This paper presents independent multi-instrument observations that address the physical mechanisms of how ULF wave associated electric fields initiate ionospheric density fluctuation and scintillation at the equator. Since the magnetic field at the equator is entirely embedded in a relatively high collision and high conductivity medium, the condition may not be possible for the geomagnetic field to fluctuate due to ULF wave activity. This implies the fluctuating electric field at the equator may not be produced through equatorial dynamo action due to fluctuating magnetic fields. Instead the electric field penetrates from high-latitudes and produce fluctuating magnetic field as well as modulates the vertical drift and hence causes the density to fluctuate at the equatorial region. We demonstrate this by estimating the ULF associated fluctuating electric field at high-latitudes and at the equatorial region by applying the appropriate attenuation factor as it penetrates to lower latitudes. The periodicity of both electric field and density fluctuations appears to be between 6 – 9 minutes, which is a typical period of

This is the author manuscript accepted for publication and has undergone full peer review but has not been through the copyediting, typesetting, pagination and proofreading process, which may lead to differences between this version and the Version of Record. Please cite this article as doi: 10.1029/2018GL078163

ULF waves in the Pc5 range. Because of its large amplitude and long periods compared to other ULF wave frequency bands, the Pc5 wave associated electric field, which can even be estimated using magnetograms with low sensitivity and low sampling rate (*e.g., 1 min*), can easily penetrate to the lower latitude region and produce significant ionospheric density fluctuations that can be strong enough to create scintillation at the equatorial region.

1. Introduction

Ultra-Low-Frequency (ULF) wave related micropulsations have been detected both on the ground and in the ionosphere. Especially, pulsations in the range of ULF Pc5 frequency ($f \approx 1.5–7$ *mHz*) are the most easily observed ULF wave, due to its large amplitude (up to some *100 nT*) and long period (several minutes) compared to other higher frequency ULF wave bands. The Pc5 pulsations are not only regularly observed near auroral latitudes [e.g., *Pilipenko et al.*, 2014a,b] but also penetrate to lower-latitudes and can be detected at mid- and low-latitudes [*e.g., Liu et al., 1993; Motoba et al.*, 2002] and even equatorial latitudes [*e.g., Yeoman et al.*, 1990; *Reddy et al.*, 1994; *Yizengaw et al.*, 2013; *Vorontsova et al.*, 2016]. Different mechanisms have been proposed to explain ULF wave penetration to lower-latitudes [*Kikuchi and Araki*, 1979; *Chi et al.*, 2001]. However, ionospheric observations of ULF wave related perturbations at low-latitudes are extremely limited, due to the lack of instrumentation in the region, and its impact at this region remains far from understood. To our knowledge, very few ULF related ionospheric studies at lower-latitudes have been performed so far. While *Patel and Lagos* [1985] reported a single Jicamarca radar observation of F-region plasma drift oscillation that was attributed to ULF wave

associated electric field fluctuation, *Reddy et al.* [1994] reported Pc5 wave related electric field oscillation at the equator as observed with a coherent VHF backscatter radar at Thumba, near Trivandrum. Recently, *Yizengaw et al.* [2013] reported Pc5 related ionospheric density and drift perturbations using Global Navigation Satellite System (GNSS) TEC and recently-installed magnetometer observations, respectively.

Although both radar and GNSS TEC exhibit significant ionospheric density fluctuations with nearly identical periodicity as the ULF wave in the Pc5 band, the physical mechanism that explain how the ULF wave modulates ionospheric density is still not fully understood. Different mechanisms for different latitude regions have been proposed; namely: (a) ion Joule heating due to ULF wave energy deposition that may shift the temperature-dependent recombination rate and cause density fluctuation coherently with ULF wave [*Pilipenko et al.*, 2014a], (b) the periodic vertical bulk motion of ionospheric plasma due to ULF wave associated fluctuating east-west electric field (E_y) that affects the vertical drift ($V_Z = E_y \cos I/B$, where I is magnetic inclination and B is the magnetic field) and eventually causes ionospheric density to fluctuate coherently with ULF waves because of the altitude dependent recombination rate [*Reddy et al.*, 1994; *Pilipenko et al.*, 2014a]. The impact of Joule heating is dominant at high-latitudes where the B-field is nearly vertical, so we do not expect it to be a dominant source of density fluctuation in the equatorial ionosphere. The latter mechanism on the other hand is a promising technique in explaining ULF wave related ionospheric density fluctuations observed at the equatorial region where the B-field is nearly horizontal and inclination angle is nearly zero degrees.

In this paper, using a combination of independent (radar, GNSS, and magnetometer) observations, we demonstrate that the ULF wave associated fluctuating electric field penetrates to lower latitudes and triggers ionospheric density irregularity and scintillation at the equatorial region. Ionospheric scintillation, which is the rapid modification of radio wave caused by small scale ionospheric irregularity, at equatorial region is usually quantified by the S4-index for amplitude scintillation.

2. Experimental Data Analysis

For this study, we used data from ground-based magnetometers that are located at different latitudes and longitudes to monitor ULF wave magnetic pulsations and their penetration to low latitudes as well as to estimate the dayside equatorial electrojet (EEJ) at the equator. We use data from magnetometers that are operated under the umbrella of African Meridian *B*-field Education and Research (AMBER) [*Yizengaw and Moldwin*, 2009] and INTERMAGNET [*Love and Chulliat*, 2003]. Detailed description of the technique that we used to identify ULF wave pulsation and to estimate the EEJ from the magnetometer observation can be found in *Yizengaw et al.* [2013] and *Yizengaw et al.* [2014], respectively. We also used the GNSS and the 250 MHz VHF receivers, operated as part of the Air Force Research Laboratory's Scintillation Network Decision Aid (SCINDA) project [*Groves et al.*, 1997] to observe density irregularity and scintillation during the presence and absence of ULF magnetic pulsations.

3. Results

We study the moderate geomagnetic storm that occurred on 12-13 September 2014, during

which sudden jump of solar wind speed (from *400 km/s* to *650 km/s*) and ram pressure (from *1 nP*a to *10 nPa*) commenced at 15:42 UT on 12 September 2014 (not shown here). We observed significantly stronger ULF wave power at high- and equatorial latitudes following the onset time of the storm. The sudden jump of solar wind ram pressure is believed to be the driving mechanism for the ULF wave excitation. The independent observations of ULF pulsations in the magnetic field and of concurrent ionospheric density fluctuations show excellent correlation, particularly in their occurrence time period and frequency range. At high-latitudes, ULF wave power appears to be strong in the Pc5 range (1-10 mHz) but is discernible up to the Pc3 range (20 *mHz* and higher). However, at low latitude regions the wave power is mostly confined between 1.5 and 8*mHz* (a Pc5 wave band) frequency band. So Pc5 wave is clearly visible at the equatorial region unlike the higher ULF frequency bands.

Figure 1 shows nightside ULF wave associated magnetic and ionospheric density fluctuations observed at equatorial latitudes following the sudden jump of the solar wind speed and ram pressure on 12 September 2014. The second and third panels from the bottom show the dynamic spectra of the north-south magnetic field component recorded at Addis Ababa in Ethiopia (38.8°E, 9.0°N geog., and 0.16°N geom.) and at Resolute Bay (94.9°W, 74.7°N geog., and 83.6°S geom.) during the 15:30-23:30 UT on 12 September. At high-latitude the wave activity is strong and wider in frequency (goes up to 20 mHz or more) but is bound within the 2-8mHz, Pc5 frequency band, at equatorial latitudes, except between 15:40-16:00UT which is right after the sudden solar wind ram pressure enhancement at 15:42UT (indicated by vertical dotted

lines). The RES and AAE stations are located at UT - 6 and UT + 3 local time zone, respectively. Therefore, for the time period covered in the plot shown in *Figure 1*, RES and AAE were in the dayside and nightside local time sectors, respectively. The solid and dashed vertical white lines in the RES and AAE plots indicate the local noon and midnight, respectively.

The second row from the top in *Figure 1* shows dynamic spectra of GNSS TEC recorded at Bahir Dar in Ethiopia (37.4°E, 11.6°N geog., and 2.6°N geom.), indicating strong ULF wave power confined between 2-7 *mHz* frequency range, which is similar to the ULF wave signatures shown on the magnetic field fluctuation observed at AAE station (second panel from the bottom). The two side-by-side panels in the second row from the top represent TEC from two sample satellites (PRNs (pseudo random numbers) 1 & 4), and the white curve in each panel depicts the vertical TEC (from the corresponding GNSS satellite) with its scale on the right side of each panel. The bottom panel shows the band-bass filtered time series of GNSS TEC for 7 different satellites. Different colors represent different GNSS satellites, and the corresponding PRNs are shown at the bottom of the panel. The black curve (with its scale at the right side) is an independently measured scintillation (S4) index. The S4-index was measured using the passive 250 MHz VHF radar located at Bahir Dar in Ethiopia (37.4°E, 11.6°N geog., and 2.6°N geom.). It is important to note that the TEC fluctuation and scintillation kick off exactly at the same time, and it was approximately 1 hr after the impact of the solar wind dynamic pressure enhancement reached at the equator.

The top panel in *Figure 1* shows the ground tracks proximity of ionospheric pierce points

from the ground-based GNSS receiver. The tracks are color coded with integrated ULF wave power (between *2 and 8mHz* frequency band) of the TEC dynamic spectra (second row from the top). The horizontal magenta dashed line indicates the location of the geomagnetic equator at the meridian of GNSS station. The start and end UT times for the period that a satellite is within the station's field of view (FOV) are marked at the entrance and exit point of each PRN ground track. The first satellite that came in-view from the northern side of the station and observed strong density fluctuations between 17:45 and 19:18UT was PRN 32. Although the ULF power appeared almost instantly at 15:42UT (the dynamic pressure sudden enhancement time), the density fluctuation as well as VHF S4-index did not start until 16:45UT. However, once the ULF power associated density fluctuation began, the GNSS satellites that came in-view at a latter local time experienced density fluctuation almost throughout their entire pass over the station. PRN 1 demonstrates this; it experienced density fluctuation throughout its pass, depicting the wide spatial area coverage of ULF wave power associated density fluctuation. However, while the VHF S4-index still showed strong scintillation activity during post-midnight sector (black curve peaked at ~22:00 UT), the GNSS density fluctuations are significantly decreased after midnight (see bottom panel in *Figure 1*). This is likely due to the fact that background ionospheric density is very low during post-midnight to detect fluctuations with GNSS frequency. The VHF S4-index also exhibited a slight enhancement right after 23:00 UT, which could be associated with a strong ULF power between 22:40 and 23:15 UT shown at the second panel from the bottom, but the GNNS density showed no fluctuation.

Similarly, the dayside ULF wave activity also causes noticeable density fluctuations at the equatorial region during strong geomagnetic storm that occurred on June 22-24, 2015 (not shown here). There is a striking difference in the TEC level of fluctuations between the absence and presence of ULF wave activity periods. However, the dayside density fluctuation was not as strong as nightside ULF wave associated density fluctuation. The ULF wave associated storm-time EEJ modulation has also been observed at the Phuket station (98.4°E, 7.9°N geog., and 0.6°S geom.) during 01:00-08:30 UT (07:30–14:30 LT) on 23 June 2015 (not shown here). The magnitude and direction of the dayside EEJ, which is directly proportional to the vertical velocity (**E**×**B** drift), are estimated using pairs of ground magnetometers located at Phuket and Bangkok (100.6°E, 14.1°N geog., and 6.2°N geom.) [*e.g., Anderson et al.*, 2002; *Yizengaw et al.*, 2011, 2012, 2014]. The nearly periodic (a few minutes) small scale EEJ fluctuations are embedded into the large-scale (an hour) fluctuations, and a bandpass filtering technique has been applied to identify the type of wave embedded into these small-scale fluctuations. The filtered dayside EEJ (not shown here) shows fluctuation with 6-9 min periodicity, which is a typical ULF wave in the Pc5 range.

Figure 2 shows the comparison of filtered TEC fluctuations (third panel from the top) with magnetic variations at RES (top panel) and AAE (second panel from the top), indicating the coherent periodicity between TEC and magnetic fluctuations. Interestingly, the time scale (6 – 8min) of TEC fluctuation is nearly the same as geomagnetic pulsations both at high- and equatorial-latitudes, and it is a typical periodicity of ULF wave in the Pc5 range. In general, this

coherent periodic TEC and magnetic fluctuations demonstrate that the magnetospheric origin ULF wave can cause not only geomagnetic but also ionospheric density fluctuations at the equator. The amplitude of the nightside ULF wave associated TEC fluctuation at the equatorial region is also significant. While the peak-to-peak amplitude of TEC oscillation at low-latitude is ΔTEC ~1.4 TECU, the magnetic pulsations at high-latitude and at equatorial region are ΔH ~ 60nT and ΔH ~ 3nT, respectively. The difference in the peak-to-peak amplitude of magnetic pulsations at high-latitude and equatorial region indicate the attenuation of ULF wave power when it penetrates to low-latitudes.

Furthermore, the cross-spectral analysis (applied to the unfiltered TEC and magnetic field data for the time period 16:30 – 20:00 UT) also confirms excellent correlation between TEC and magnetic variations as shown in the bottom panel of *Figure 2*. The spectral power peaks of TEC and magnetic fluctuations occur at the same frequencies (f ~ *1.5 mHz, 2.3 mHz, 3 mHz, 3.6 mHz*) that are depicted by dotted vertical green lines. Different multiplication factors (shown in the figure) are applied to accommodate the spectral powers of TEC and magnetic variations in same panel with the same vertical scale. The correlation coefficients of the spectral coherency of TEC variation at low-latitude with the magnetic fluctuations at high-latitude and at the equator are $\gamma \sim 0.78$ and $\gamma \sim 0.86$ respectively.

4. Discussion and Conclusion

Several mechanisms have been proposed to explain the physics behind the ULF wave associated ionospheric density fluctuation observed at low-latitude region. *Poole et al.* [1988]

proposed four mechanisms that are responsible for ULF wave related density oscillation; namely: (1) the change in refractive index due to the time varying magnetic field magnitude, (2) the east-west electric field fluctuation due to the ULF associated current fluctuation, (3) the compression and rarefaction of plasma due to the ULF wave related compression and rarefaction of the magnetic field, and (4) the variation of photochemical reaction. However, the contribution of the first and fourth mechanisms to the density fluctuation is insignificant, indicating that either the second or third mechanisms could be the dominant source of ULF related density fluctuation at the equator [*e.g., Poole and Sutcliffe*, 1987; *Poole et al.*, 1988; *Liu and Berkey*, 1994; *Reddy et al.*, 1994]. Thus, to identify the favorable mechanisms that explain the ULF related density fluctuation at the equator, we investigated the second and third techniques by looking at several case studies for different time periods.

Liu and Berkey [1994], using the relationship between ionospheric electric field and magnetic field fluctuations given by *Hughes* [1974] and by representing the notation $\partial/\partial t = -i\omega$, estimated the amplitude of ionospheric east-west electric field fluctuation mathematically as:

$$\delta E_y = -\frac{\varepsilon\,\delta B_x}{f\cos\left(1/(\sqrt{\varphi f^2+1})\right)} + \frac{i\varepsilon\,\delta B_x \ln\left(\varphi f^2+1\right)}{2f} \quad (1)$$

where $\varepsilon = k^2c^2H/2\pi$, $\varphi = (2\pi/\mu_o\sigma_g c^2)^2$, H is atmospheric scale height, σ_g is atmospheric conductivity near the ground, c and μ_o are speed of light and permeability constant in free space, k is the wave number of the ULF wave perturbation, δB_x is the magnetic pulsation observed at the ground, and f is the ULF wave frequency.

For this study, we used the same mathematical expression to estimate the amplitude of ionospheric fluctuating electric field from the pulsation of geomagnetic field observed at the ground. Thus, by considering the typical values of atmospheric scale height ($H = 8.5\ km$) and conductivity ($1.6 \times 10^{-14}\ ohm/m$) near the ground, we estimated the east-west electric field fluctuations that are associated with the ULF wave related magnetic pulsation. *Figure 3* shows electric field fluctuation estimated at high-latitude (top panel) and at the equator (middle panel) using *equation 1*. The magnitude of the fluctuating electric field at the equator is much less than that of high-latitude electric field. The bottom panel indicates the same as ionospheric density fluctuation and scintillation shown in *Figure 1*. Both TEC fluctuation and S4-index enhancement start at the same time, which is about 1 hr later from the starting time of the ULF pulsation signature on the geomagnetic field and thus on the east-west electric field. The ULF power appeared at the equator almost instantly at 15:42UT as shown in *Figure 1* (second panel from the bottom), but the density fluctuation from the first in-view GNSS satellite (PRN 32) as well as VHF S4-index did not start until 16:45UT. This nearly an hour time gap is a typical time delay between the start of electrodynamic impact on the ionosphere (by imposing the vertical bulk movement of the ionosphere) and the response of F-region plasma Rayleigh-Taylor instability growth rate [*e.g., Sultan*, 1996].

The question is what is the physical mechanism that the ULF wave can cause strong east-west electric field oscillation at the equatorial region and lead to the formation of such strong density irregularity and thus scintillation? It is obvious that ULF wave causes electric field

perturbation in the ionospheric dynamo region at all latitudes when mapped along the field lines [*Hughes*, 1974; *Reddy et al.*, 1994; *Yizengaw et al.*, 2013]. However, this conclusion may not be true all the time due to a simple factual difference between ionospheric region in the high-latitude and equatorial region. Unlike the high-latitude geomagnetic field orientation and its surrounding ionospheric condition, the geomagnetic field lines in the equatorial region are entirely embedded in a relatively high collision and high conductivity medium. This prohibits the field lines in the equatorial ionosphere to support the ULF wave triggered oscillation with significant amplitude. This means the fluctuating electric field that has been often observed at the equator cannot be produced due to a locally initiated magnetic field pulsation. If it is not due to the ULF waves that penetrate to the equatorial ionosphere and makes field lines to oscillate at the rate of ULF wave frequencies, then where does such a strong magnetic and thus electric field perturbations come from?

The high-latitude situation allows, the damped haydromagnetic ULF waves to modulate the current system and produce significant amplitude oscillations onto the magnetic and electric fields [*Hughes*, 1974]. It is also well-known observationally that the storm and substorm-related electric field at high latitudes penetrate to low latitudes but with significant attenuation [*Reddy et al.*, 1994; *Kikuchi et al.*, 2000]. The ULF associated fluctuating electric field at high-latitude region also penetrate in the same way to low-latitudes through the TM0 (zero order transverse magnetic) mode waves in the Earth-ionosphere waveguide [*e.g., Kikuchi and Araki*, 1979; *Yizengaw et al.*, 2016]. The geomagnetic field oscillation observed at the equator is thus assumed to be caused by

the current driven by this penetrated ionospheric electric field. However, due to the ionospheric attenuation factor, the magnitude of the fluctuating east-west electric field decreases as it penetrates to lower latitudes as shown in *Figure 3*. *Kikuchi* [2014] examined possible attenuation factors of electric field penetration, and suggested that could be due to the geometrical attenuation and finite conductivity of the ionosphere. They concluded that during nighttime (in an extreme case of poorly conducting ionosphere) the former and the latter factors allow about 10% and 85% of the polar electric field to reach the equator, respectively. Although the attenuation factor due to finite conducting ionosphere increases during daytime, where ionospheric conductivity is higher, the substantial attenuation happens to be due to the geometrical attenuation which is consistent with our observations and with *Kikuchi* [2014]. In *Figure 3* the fluctuating electric field estimated at the equator, using the observed magnetic field pulsation, is on the order of 0.15-0.25 mV/m, which is nearly 10% of the electric field estimated at high-latitude region. This also has been visible in the peak-to-peak amplitude difference between magnetic fluctuations at high- and low-latitudes (see *Figure 2*). However, for the dayside (when the second attenuation factor also contribute significantly due to the highly conducting ionosphere), the attenuation factor becomes a bit higher. Even so, significant amplitude electric field penetrates to low-latitude region, which is also amplified by EEJ at the equator, and produce density fluctuation on the dayside (not shown here).

The corresponding vertical drift oscillation at the equator (see *Figure 3*) has an amplitude of 2.5 - 7.0 m/s, which is 25 -50% of the typical quiet time dayside maximum value of the vertical

drift. This is consistent with *e.g., Vikramkumar et al.* [1987] and *Reddy et al.* [1994]. However, if the magnetospheric source of ionospheric electric field extends to lower L-values (lower than the corresponding auroral latitudes), then it penetrates to the equatorial ionosphere with a smaller degree of attenuation. This is because it skips an extra attenuation factor arising from the highly conducting region in the auroral belt. Therefore, depending upon the strength of the ULF wave power, the ULF associated fluctuating ionospheric electric field can introduce substantial modulations in the vertical drift. The density fluctuation and scintillation that we observed on the ground were then taken to be due to the fluctuating vertical component of the bulk motion of the ionosphere caused by the **ExB** drift associated with the oscillating electric field in the F-region. Interestingly, the density fluctuation at the equatorial region also occur coherently with the magnetic fluctuations at high- and low-latitudes (see *Figure 2*), demonstrating that the magnetospheric origin ULF wave activity modulate high-latitude electric field that can penetrate to equatorial latitudes and cause density irregularities in the ionosphere. This demonstrates that the second mechanism (among the four possible mechanisms suggested by *Poole et al.* [1988]) is the dominant mechanism for the density fluctuation often observed at the equator. In the dusk to midnight region, where the background density is weaker, ionospheric plasma layers can be easily driven up-and-down by small magnitude of fluctuating vertical drift. This create favorable conditions for the development of density fluctuation and scintillation, indicating that Solar wind driven ULF waves could also be a driving mechanism for the formation of scintillation.

In conclusion, the magnetospheric origin ULF wave associated high-latitude electric field

penetrate to lower-latitudes and cause ionospheric density to fluctuate and even form scintillation at the equatorial region. Equatorial scintillation is known as event driven by either an internal Ionosphere-Thermosphere process, typically triggered by gravity waves seeding [*e.g., Hysell et al.,* 1990], or due to storm time strong magnetospheric origin dawn-to-dusk electric field penetration to lower-latitudes in the case of southward turning of IMF Bz [*e.g., Basu et al.,* 2007]. In this study, we have demonstrated, to our knowledge - for the first time, a direct source and effect relationship between Solar wind driven ULF wave power and the density fluctuation/scintillation activity at the equatorial region. The mechanism that produces such density fluctuation and scintillation at the equator could be due to a ULF wave associated fluctuating ionospheric electric field that penetrates from high-latitude region. This has been unequivocally confirmed with the cross-spectral analysis that shows the spectral power peaks occur 1.5 - *4mHz* frequency band, which is in the typical Pc5 range. The spectral coherency correlation between TEC and magnetic fluctuations is also high ($\gamma \sim 0.86$). Since Pc5 waves have large amplitudes and long periods compared to other ULF wave frequency bands, the Pc5 wave associated electric field can easily penetrate to lower latitude region and produce significant ionospheric density fluctuation that can be strong enough to create scintillation at the equatorial region. Such density fluctuations have been often observed at the equatorial region, though they are sometimes misinterpreted as plasma waves of longer periods generated by gravity waves.

Acknowledgment

This work has been partially supported by AFOSR (FA9550-15-1-0399), NSF (AGS145136 and AGS1450512), and NASA (13-SRITM13_2-0011) grants. The authors are indebted to the SCINDA team for the GPS and VHF data resources they made available to this study. We also thank the INTERMAGNET global team for the magnetometer data. The solar wind data was obtained from the CDAWeb database. EY thanks the ISSI-Bern International Team of "*Ionospheric Space Weather Studied by RO and Ground-based GNSS TEC Observations" (the team leader J. Y. Liu*) for valuable discussion that he has about part of the result included in this paper.

Reference

Anderson, D., A. Anghel, K. Yumoto, M. Ishitsuka, and E. Kudeki (2002), Estimating daytime vertical ExB drift velocities in the equatorial F-region using ground-based magnetometer observations, *Geophys. Res. Lett.*, *29*(12), 1596, doi:10.1029/2001GL014562.

Basu, S., Su. Basu, F. J. Rich, K. M. Groves, E. MacKenzie, C. Coker, Y. Sahai, P. R. Fagundes, and F. Becker-Guedes (2007), Response of the equatorial ionosphere at dusk to penetration electric fields during intense magnetic storms, *J. Geophys. Res.*, *112*, *A08308, doi:*10.1029/2006JA012192.

Boudouridis, A. and E. Zesta (2007), Comparison of Fourier and wavelet techniques in the determination of geomagnetic field line resonances, *J. Geophys. Res., 112*, A08205, 2006JA011922.

Chi, P. J., C. T. Russell, J. Raeder, E. Zesta, K. Yumoto, H. Kawano, K. Kitamura, S. M. Petrinec, V. Angelopoulos, G. Le, M. B. Moldwin (2001), Propagation of the preliminary reverse impulse of sudden commencements to low latitudes, *J. Geophys. Res.*, 106, 18,857–18,864.

Groves, K. M., et al. (1997), Equatorial scintillation and systems support, *Radio Sci., 32(5), 2047–2064, doi:10.1029/97RS00836.*

Hughes, W. J. (1974), The effect of the atmosphere and ionosphere on long period magnetospheric micropulsations, *Planet. Space Sci.* 22(8), 1157-1172.

Hysell, D. L., M. C. Kelley, W. E. Swartz, and R. F. Woodman (1990), Seeding and layering of equatorial spread *F* by gravity waves, *J. Geophys. Res.*, *95(A10*), *17253–17260*, doi:10.1029/JA095iA10p17253.

Kikuchi, T. (2014), Transmission line model for the near-instantaneous transmission of the ionospheric electric field and currents to the equator, *J. Geophys. Res.*, *119*, 1131–1156, doi:10.1002/2013JA019515.

Kikuchi, T., and T. Araki (1979), Horizontal transmission of the polar electric field to the equator, *J. Atmos. Terr. Phys.*, 41, 927– 936.

Kikuchi, T., H. Lühr, K. Schlegel, H. Tachihara, M. Shinohara, and T.-I. Kitamura (2000), Penetration of auroral electric fields to the equator during a substorm, *J. Geophys. Res.*, 105, *23,251–23,261, doi:10.1029/2000JA900016.*

Liu, J. Y. and F. T. Berkey (1994), Phase relationships between total electron content variations, Doppler velocity oscillations and geomagnetic pulsations, *J. Geophys. Res.*, 99(A9), 17539-17545.

Liu, J. Y., Y. N. Huang, and F. T. Berkey (1993), The Phase Relationship between ULF Geomagnetic Pulsations and HF Doppler Frequency Shift Oscillations on March 24, 1991, *J. Geomag. Geoelectr. 45*, 109-114

Love, J. J. and A. Chulliat (2013), An international network of magnetic observatories, *Eos, Trans. AGU*, 94(42), 373-374.

Motoba, T., T. Kikuchi, H. Lühr, H. Tachihara, T.-I. Kitamura, K. Hayashi, and T. Okuzawa (2002), Global Pc5 caused by a *DP* 2–type ionospheric current system, *J. Geophys. Res., 107(A2), doi:10.1029/2001JA900156.*

Patel, V. L., and P. Lagos (1985), Low-frequency fluctuations of the electric field in the equatorial ionosphere, *Nature 313(6003), 559-560*.

Pilipenko, V., V. Belakhovsky, A. Kozlovsky, E. Fedorov, and K. Kauristie (2014), ULF wave modulation of the ionospheric parameters: Radar and magnetometer observations, *J. Atmos. Sol. Terr. Phys.*, 108, 68–76.

Pilipenko, V., V. Belakhovsky, D. Murr, E. Fedorov, and M. Engebretson (2014), Modulation of total electron content by ULF Pc5 waves, *J. Geophys. Res.*, 119, 4358–4369, doi:10.1002/2013JA019594.

Poole, A. W. V. and P. R. Sutcliffe (1987), Mechanisms for observed total electron content pulsations at mid latitudes, *J, Atmos. Terr. Phys., 49, 231-236*.

Poole, A. W. V., P. R. Sutcliffe, and A. D. M. Walker (1988), The relationship between ULF geomagnetic pulsations and ionospheric Doppler oscillations: Derivation of a model, *J. Geophys. Res.*, 93(A12), 14656-14664.

Reddy, C. A., S. Ravindran, K. S. Viswanathan, B. V. K. Murthy, D. R. K. Rao, T. Araki (1994), Observations of Pc5 micropulsation-related electric field oscillations in equatorial ionosphere, *Ann. Geophys.*, 12(6), 565-573.

Saito, T. (1969), Geomagnetic pulsations, *Space Sci. Rev.* 10(3), 319-412.

Strumik, M., V. Roytershteyn, H. Karimabadi, K. Stasiewicz, M. Grzesiak, and D. Przepiórka (2015), Identification of the dominant ULF wave mode and generation mechanism for obliquely propagating waves in the Earth's foreshock, *Geophys. Res. Lett., 42, 5109–5116, doi:10.1002/2015GL064915.*

Vikramkumar, B. T., P. B. Rao, K. S.Viswanathan, C. A. Reddy (1987), Electric fields and currents in the equatorial electrojet deduced from VHF radar observations-III. Comparison of observed ΔH values with those estimated from measured electric fields, *J. Atmos. Terr. Phys. 49(2), 201-207.*

Vorontsova, E., V. Pilipenko, E. Fedorov, A. K. Sinha, and G. Vichare (2016), Modulation of total electron content by global Pc5 waves at low latitudes, *Adv. Space Res., 57*, N1, 309-319.

Yeoman, T. K., M. Lester, D. Orr, H. Luehr (1990), Ionospheric boundary conditions of hydromagnetic waves - The dependence on azimuthal wavenumber and a case study, *Plan. Space Sci.* 38, 1315-1325.

Yizengaw, E., and M. B. Moldwin (2009), African Meridian B-field Education and Research (AMBER) Array, *Earth Moon Planet,104(1), 237-246, doi:10.1007/s11038-008-9287-2.*

Yizengaw, E., E. Zesta, C. M. Biouele, M. B. Moldwin, A. Boudouridis, B. Damtie, A. Mebrahtu, F. Anad, R. F. Pfaff, and M. Hartinger (2013), Observations of ULF wave related equatorial electrojet fluctuations, *J. Atmos. Solar-Terr. Phys., 103, 157-168.*

Yizengaw, E., E. Zesta, M. B. Moldwin, B. Damtie, A. Mebrahtu, C. E. Valladares, and R. F. Pfaff (2012), Longitudinal differences of ionospheric vertical density distribution and equatorial electrodynamics, *J. Geophys. Res.,117, A07312, doi:10.1029/2011JA017454.*

Yizengaw, E., M. B. Moldwin, A. Mebrahtu, B. Damtie, E. Zesta, C. E. Valladares, and P. H. Doherty (2011), Comparison of storm time equatorial ionospheric electrodynamics in the African and American sectors, *J. Atmos. Solar-Terr. Phys., 73(1), 156-163*.

Yizengaw, E., M. B. Moldwin, E. Zesta, C. M. Biouele, B. Damtie, A. Mebrahtu, B. Rabiu, C. E. Valladares, and R. Stoneback (2014), The longitudinal variability of equatorial electrojet and vertical drift velocity in the African and American sectors, *Ann. Geophys., 32, 231–238*.

Yizengaw, E., M. B. Moldwin, E. Zesta, M. Magoun, R. Pradipta, C. M. Biouele, A. B. Rabiu, O. K. Obrou, Z. Bamba, and E. R. de Paula (2016), Response of Equatorial Ionosphere to the Geomagnetic *DP*2 current system, *Geophys. Res. Lett. 43, doi:10.1002/2016GL070090.*

Figure Caption:

Figure 1. The top panel shows the ground tracks of GNSS ionospheric pierce points, color coded with integrated ULF wave power (between *2 and 8mHz* frequency band) of the dynamic spectara of GNSS TEC (second panel), and horizontal magenta dashed line indicates the geomagnetic equator at the meridian of GNSS station. The third and fourth panels from the top indicate dynamic spectra of the north-south geomagnetic field component recorded at Resolute Bay and Addis Ababa. Bottom panel present the filtered GNSS TECs (different colors indicate different GNSS satellites in which the corrosponding PRNs are given at the bottom). The black curve (with the scale at the right side) shows S4-index recorded by 250MHz VHF radar at Bahir Dar.

Figure 2. Filtered x-component magnetic fluctuations at high-latitude (top panel) and equatorial region (second panel from the top). Third panel from top presents filtered TEC fluctuation at equatorial region. The cross-spectral analysis of magnetic field at high-latitude (black curve) and equatorial region (blue curve) as well as TEC at the equatorial region (red curve) observed from 16:30 to 20:00 UT. While the cross-spectral correlation between TEC at the equator and magnetic at high-latitude is $\gamma \sim 0.78$ (given in blue), the TEC and magnetic at the equator is even higher $\gamma \sim 0.86$ (given in red). The green dotted vertical lines indicate the frequencies where spectral peaks of TEC and magnetic occur coherently.

Figure 3. Shows electric field fluctuation estimated at high-latitude (top panel) and at the equator (middle panel). Bottom panel is as for Figure 1's bottom panel.

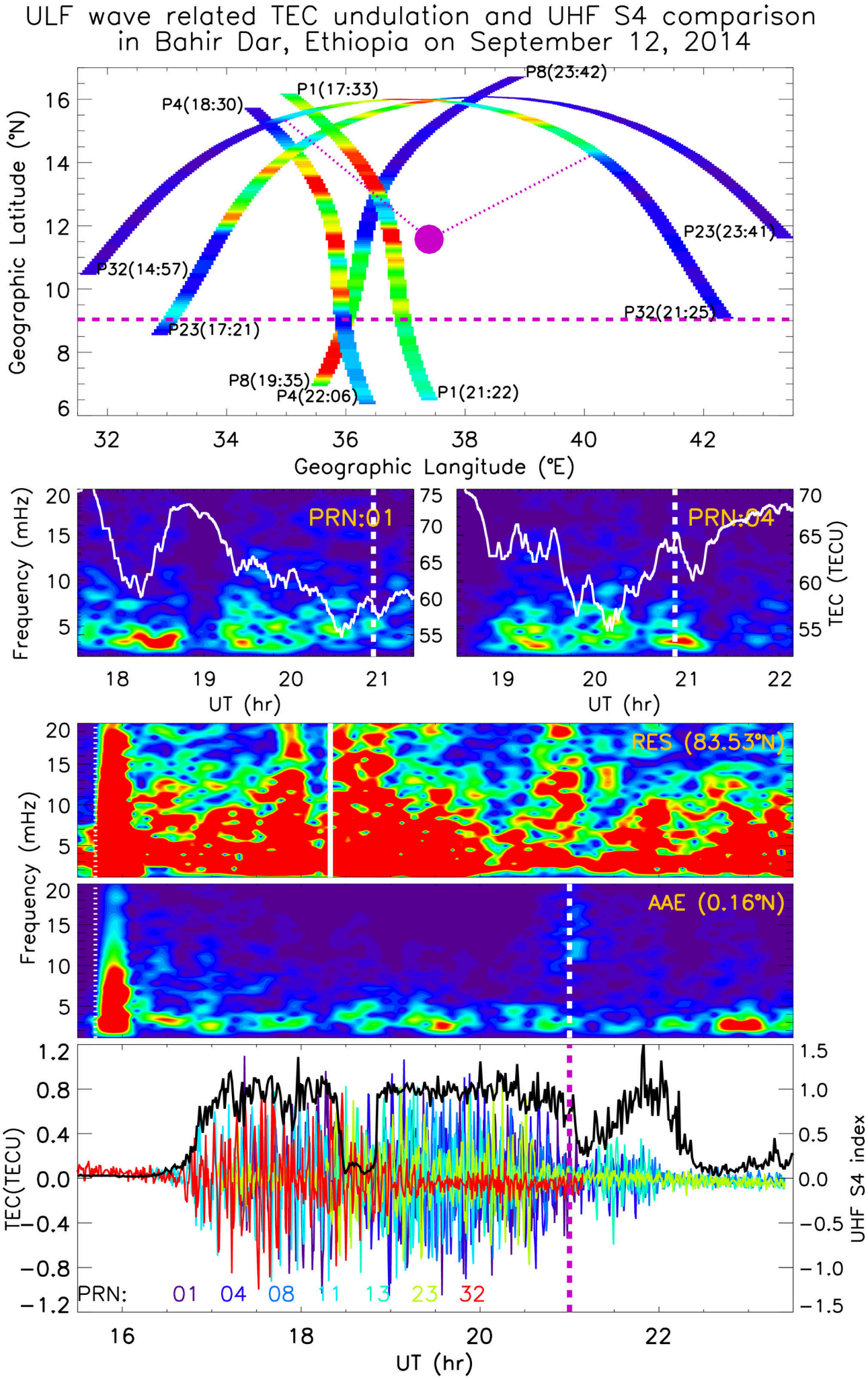

2018gl078163-f01-z-eps

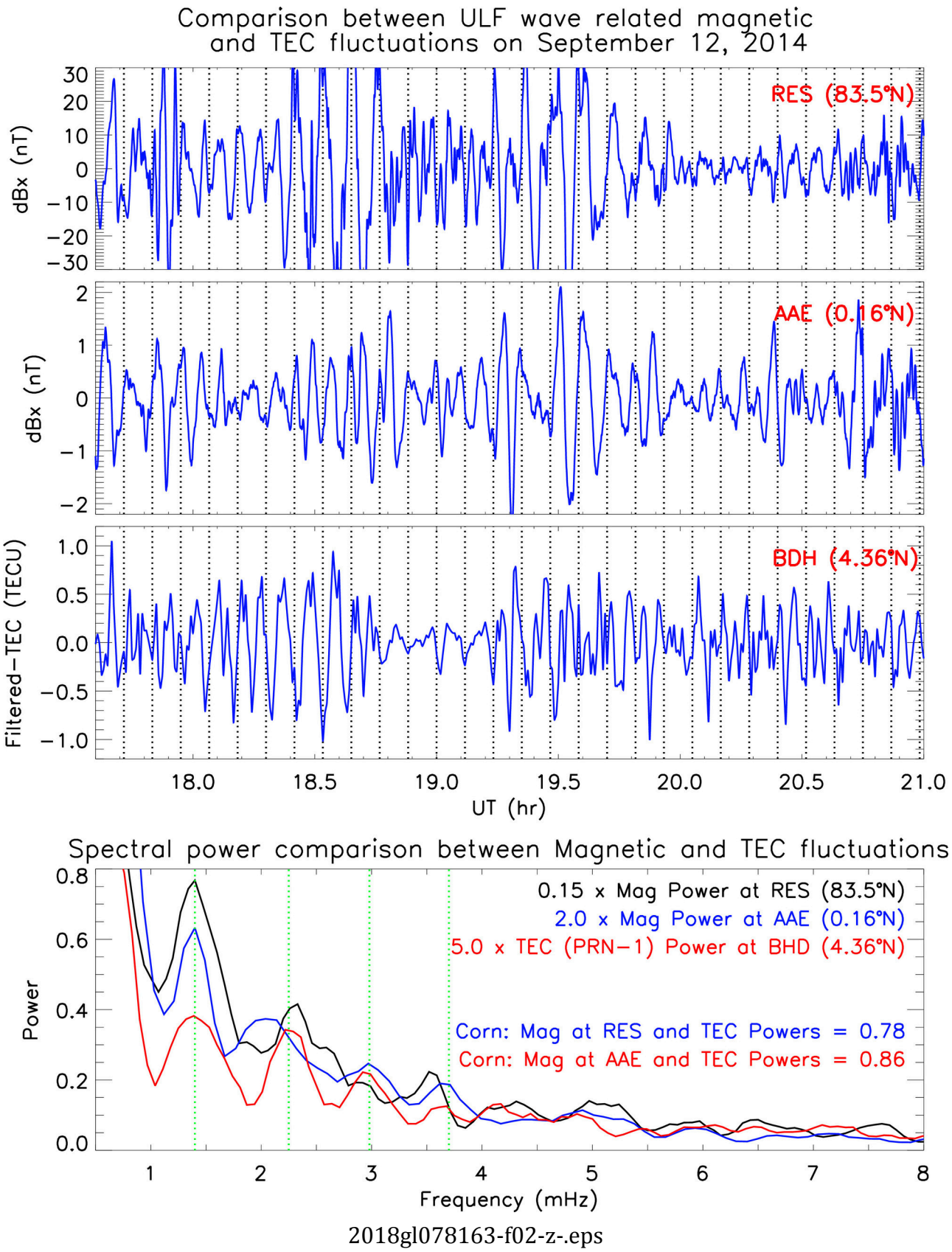

2018gl078163-f02-z-.eps

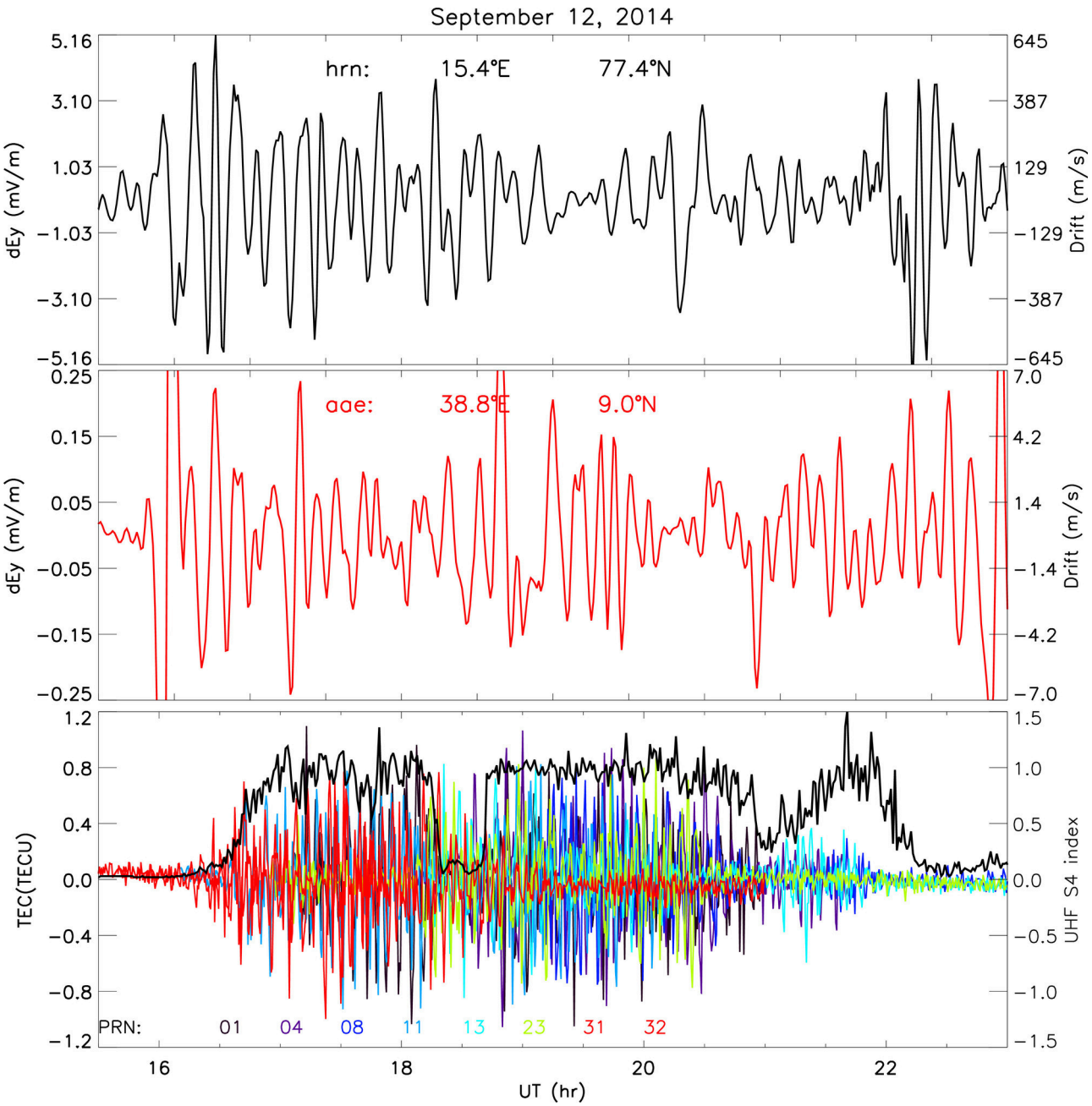

2018gl078163-f03-z-.eps